The Magnitude and Mechanism of Charge Enhancement of CH··O H-bonds

Upendra Adhikari and Steve Scheiner*
Department of Chemistry and Biochemistry
Utah State University
Logan, UT 84322-0300

*email: steve.scheiner@usu.edu
phone 435-797-7419

ABSTRACT

Quantum calculations find that neutral methylamines and thioethers form complexes, with N-methylacetamide (NMA) as proton acceptor, with binding energies of 2-5 kcal/mol. This interaction is magnified by a factor of 4-9, bringing the binding energy up to as much as 20 kcal/mol, when a CH_3^+ group is added to the proton donor. Complexes prefer trifurcated arrangements wherein three separate methyl groups donate a proton to the O acceptor. Binding energies lessen when the systems are immersed in solvents of increasing polarity, but the ionic complexes retain their favored status even in water. The binding energy is reduced when the methyl groups are replaced by longer alkyl chains. The proton acceptor prefers to associate with those CH groups which are as close as possible to the S/N center of formal positive charge. A single linear CH··O H-bond is less favorable than is trifurcation with three separate methyl groups. A trifurcated arrangement with three H atoms of the *same* methyl group is even less favorable. Various means of analysis, including NBO, SAPT, NMR, and electron density shifts, all identify the $^+$CH··O interaction as a true H-bond.

keywords: $^+$S-CH··O, $^+$N-CH··O, trifurcated H-bond, solvent effects, NBO, SAPT

INTRODUCTION

Of all the noncovalent forces that occur between separate molecules, or between various segments of the same molecule, H-bonding has arguably been the most intensively studied over the years. Decades of research have provided a wealth of information [1-4] about the underlying nature of the attraction, and of some of the accompanying phenomena. For example, the formation of a A-H···D H-bond typically results in a small elongation of the A-H covalent bond, with an associated red shift of its stretching frequency.

Recent years have witnessed a broadening of the concept of H-bonding in a number of directions [5, 6]. For example, the electron donor D can be a H atom with a partial negative charge in what is usually called a dihydrogen bond [7-11]. Or the electrons can come not from a D lone pair, but rather from a π bond [7, 12-15]. Another extension of the H-bond concept arises from the notion that the proton donor A atom can be less electronegative than the usual O, N, or F atoms. In addition to S or Cl [16-18], C has also been shown [19-28] to participate in H-bonds as the proton donor. In an interesting twist, certain CH··O H-bonds violate the usual rule of a red shifted C-H stretching frequency, with this mode shifting instead to higher frequencies [29-36].

Most of the extensions mentioned above are weaker than standard H-bonds, sometimes pushing the boundaries of the lower limit of strength. On the other end of the spectrum are very strong H-bonds, in which one of the two subunits carries an electric charge [37-40]. The neutral water dimer, for example, is bound by some 5 kcal/mol, but if one of the two water molecules is replaced by either OH^- or H_3O^+, the interaction energy climbs [41-47] by a factor of 5-8. It is natural to wonder then whether such a charge-enhanced interaction energy can transform a weak H-bond such as CH··O into a much stronger one. And indeed, there is some evidence in the literature that this might be the case. Placing a negative charge on the proton acceptor [48-56] seems to cause a substantial strengthening of the attractive force within the dimer.

Likewise, adding a positive charge to the proton donor appears to have a comparable strengthening effect upon the H-bond. This phenomenon finds especial importance in the realm of biomolecular structure and function. As one example, the CH of a protonated Lys has been observed to attract a Trp sidechain [57]. Upon acquiring some charge from a nearby metal cation, the imidazole sidechain of a His residue forms CH··O H-bonds with heightened frequency of occurrence, as judged by analysis of the protein data bank [58]. The large number of CH··O H-bonds around the Cu coordination site of

amicyanin [59] suggested that charge imparted by metal-coordination applies more generally to other CH donors as well.

One interesting case study arises in the activity of a particular class of enzymes. The Trievel group's delving into the mechanism of lysine methyltransferases and demethylases [60-64] has revealed strong evidence that one or more CH··O H-bonds involving a cationic proton donor play an important role in their functioning. These donors involve either S (as in S-adenosyl-L-methionine, i.e. AdoMet) or N (lysine) as the center of positive charge (which partially motivates the model systems discussed below). However, the experimental data have not been capable of providing certain information that would aid in our understanding of how the enzymes function. For example, it is unclear whether one or more H atoms of each methyl group engage in H-bonding with a single acceptor atom. Nor has it been possible to extract the energetics of any individual CH··O interaction, an important consideration in terms of whether such bonds can hold the appropriate residues in position for enzymatic function and how they might compete with other potential H-bonds.

Quantum chemical methods offer the potential to address these issues with some clarity. One of the earliest related studies, limited to a very small basis set [65], observed that the methyl group of a cationic system could form H-bonds as strong as 15 kcal/mol with a neutral proton acceptor. Kim et al [66] later showed that protonated NH donors form H-bonds as strong as 20 kcal/mol with water, but that $^{+}$CH donors are not far behind with a binding energy of 10 kcal/mol; H-bonds of these same donors with the π system of benzene were slightly weaker. The superiority of NH over CH, even in a charged situation, was verified by Cannizzaro and Houk [67] using esters as O proton acceptors. Nonetheless, a complex containing only $^{+}$CH··O type bonds still provided a very strong interaction of some 13 kcal/mol. When amplified by a positive charge, the $C^{\alpha}H$ of a lysine model was found [68] to engage in a CH··O H-bond of some 4.9 kcal/mol, even though the center of positive charge was well removed from the bridging proton by several intervening methylene groups. With respect to aryl protons, benzene cation engages in a $^{+}$CH··O H-bond with water, with binding energy of 11.4 kcal/mol [69]. A single aryl CH of methylpyridinium forms a CH··O bond with an ester [70] of 7.5 kcal/mol, raised to 10.0 kcal/mol when this bond is complemented by a second CH··O involving a methyl H. The magnifying effect of charge was evident also [71] in the CH··O H-bond energies of imidazole with water, which jumped from 2.4 kcal/mol when imidazole was neutral up to 11.3 kcal/mol when protonated. This result was later confirmed by Schmiedekamp and Nanda [58] who extended the concept of positive charge to the proximate positioning of a cationic metal. Along a similar vein, the effects of charge were manifest

when the cationic imidazole donor $^{+}$CH··O H-bond supplanted a neutral NH··O bond as it led to triple helical structure [72] of 1-acetamido-3-(2-pyrazinyl)-imidazolium.

While certainly providing some tantalizing glimpses into the magnification of CH··O H-bond strength, the body of past calculations of charge-activated CH··O H-bonds is not as thorough nor as robust as it might be. In particular, it leaves a number of questions only partially answered. Consider the general case where one or more alkyl groups R, each containing a number of potential CH donors, are bound to a central atom X, and the entire XR_n^+ system bears an overall positive charge. By just how much does the formal positive charge amplify the strength of the CH··O H-bonding to a proton acceptor, and how is the H-bond strength affected by the identity of the central atom X? Is the interaction weakened as the CH donor moves further along the alkyl group from the center of positive charge, and if so by how much? How sensitive is the H-bond to the linearity of the CH··O arrangement; are multiple bent CH··O bonds superior to a single linear bond? What is the effect of immersion of the system into a solvent of varying polarity? And as a particularly important question, can charge-magnified CH··O interactions compete effectively with neutral H-bonds of the conventional OH··O or NH··O sort?

The present work represents an attempt to answer these questions in a systematic manner. Quantum calculations are applied to systems that pair cationic XR_n^+ with the O atom of N-methylacetamide (NMA) as the common proton acceptor. The latter was chosen in part for its similarity to the peptide unit that is so pervasive in proteins. The central X atom was taken as first S and then N, so as to explore both chalcogen and pnicogen types. And as noted above, both of these atoms are of particular relevance with regard to possible $^{+}$CH··O H-bonds within the transferase class of enzymes. Alkyl groups R were varied in length from methyl up to n-butyl which permit an exploration of the way in which distance from the central atom might affect the proton-donating potency of CH. The entire set of cationic systems are compared with their neutral analogues, to obtain direct estimates of the effects of charge. Finally, the systems are immersed in a variety of solvents, to assess how the results might be affected by the polarity of the surrounding medium. The results of this work will not only be of fundamental value in understanding ionic CH··O H-bonds in general, but of immediate use in better unraveling the mechanism of the methyl transferase enzymes as the model systems chosen bear a close resemblance to the actual enzymatic complexes.

COMPUTATIONAL METHODS

All calculations were performed via the Gaussian 09 package [73]. The MP2/aug-cc-pVDZ level of theory was chosen for its ability to handle H-bonding interactions at a high level of accuracy [55, 74-79].

The M06-2X density functional [80] was used for some of the larger systems. Not only was this method developed in order to handle intermolecular interactions, but it has shown good reliability in the past [81-84] when dealing specifically with CH H-bonds. In addition, as discussed below, the H-bond properties computed by M06-2X/6-31+G** were directly compared with MP2/aug-cc-pVDZ for the particular systems of interest here, and shown to be in close coincidence.

Binding energies were defined as the difference between the energy of the complex and the sum of energies of optimized monomers and were corrected for basis set superposition error by the counterpoise procedure [85]. (Of all the possible conformers of each trialkylated monomer, the minimum chosen was that which most closely matched its structure in the complex, so as to avoid comparing unlike conformers.) All minima were verified as having no imaginary frequencies. Natural Bond Orbital (NBO) analyses [86, 87] were performed via the procedures contained within Gaussian. The binding energies of complexes were decomposed by symmetry adapted perturbation theory [88] (SAPT) via the Molpro [89] set of codes. The effects of solvation were estimated using the conductor polarized continuum model (CPCM) [90]. NMR chemical shifts were calculated using the GIAO [91, 92] method, as coded in the Gaussian-09 program.

RESULTS

N-methyl acetamide (NMA) as common proton acceptor was paired with the neutral $S(Me)_2$ and $N(Me)_3$ molecules, and then with the corresponding $S(Me)_3^+$ and $N(Me)_4^+$ cations. Full geometry optimizations were carried out at the MP2/aug-cc-pVDZ level of theory, and led to the structures illustrated in Fig 1. It may be noted first that these global minima all share one important characteristic: the NMA O atom interacts with as many methyl groups as possible. In other words, there are three CH··O bonds, each to a different methyl group for all complexes, with the exception of $S(CH_3)_2$ where there are only two such methyl groups present. The θ(CH··O) angles of these H-bonds all show a good deal of deviation from its ideal of 180°, with angles in the 137-150° range. Such nonlinearities are necessary in order to form multiple CH··O bonds with a single O atom. It might be emphasized that the three concurrent H-bonds formed by the O atom in most of these complexes contradicts the notion that the presence of only two O lone pairs might similarly limit the number of potential H-bonds.

The counterpoise-corrected binding energies are displayed as the large blue numbers in Fig 1, and illustrate the magnification that is associated with the formal positive charge. The two neutral complexes are bound by 2-5 kcal/mol, with $S(CH_3)_2$ forming a stronger complex than does $N(CH_3)_3$. Along with its stronger binding, the CH··O H-bonds are shorter in the former case. The $N(CH_3)_3$ complex is not symmetric, as one of the CH··O bonds is some 0.3 Å longer than the other two. Note, however, the much

shorter H-bonds in the two charged complexes in Figs 1b and 1d, with distances of about 2.2 Å. Along with this bond contraction comes a magnification of the binding energy to about 20 kcal/mol, with the S-containing complex again somewhat more strongly bound than its N analogue. The addition of the positive charge to the proton donor molecule enhances the binding energies by some 16 kcal/mol, representing a fourfold increase for S and ninefold for N.

Solvent Effects

It is generally thought that a polar solvent ought to weaken H-bonds, particularly those of ionic type. The effects of solvent were considered by applying the CPCM method which surrounds each system by a polarizable continuum of dielectric constant ε. The systems in Fig 1 were each subjected to a full geometry optimization in each solvent chosen, and again the identity as a minimum was verified by all positive vibrational frequencies. The binding energies of each complex are plotted against the Onsager function $F_o = (\varepsilon - 1)/(\varepsilon + 2)$ [93] in Fig 2 where yellow and blue lines indicate S and N complexes, respectively, with solid and broken curves designating cationic and neutral complexes. For purposes of comparison with a paradigmatic H-bond, the binding energy of the water dimer is included as the solid red curve. $F_o = 0$ for the gas phase, where ε = 1, and this quantity rises asymptotically as the polarity increases, reaching its maximum of 0.963 for water where ε=78.

Examination of Fig 2 confirms that the interaction energy diminishes as the solvent becomes more polar. This relationship is largely a linear one, particularly for the neutral systems. It is evident that the charged complexes are more sensitive to solvent polarity, diminishing more quickly with F_o. Taking the cationic sulfonium S complex as an example, its binding energy decreases from 20.6 kcal/mol in the gas phase down to 12.8 kcal/mol when ε = 2.0 and then further to a minimum of 4.6 kcal/mol in aqueous solvent. The decrease in the neutral complex of thioether $S(Me)_2$ is more gradual, dropping from 4.9 kcal/mol at ε = 1 to 2.3 kcal/mol at ε = 78. Due to the higher sensitivity of the charged complexes to solvent polarity, as ε rises the energetic advantage of these ionic systems vs. the neutral complexes diminishes. Yet even for highly polar solvents, the cations form stronger H-bonds than do the neutral proton donors. In fact, even for aqueous solvation, the binding energies of the two charged complexes are twice that of their neutral parallels.

As the CH··O H bond weakens in more polar solvents, the two monomer units are drawn slightly further apart, in both neutral and charged complexes. The H-bond distance increases by ~0.1 Å for S complexes and ~0.2 Å for N complexes as ε climbs from 1 to 78. Surprisingly the change in H bond distance is approximately the same for neutral and cationic complexes, despite the higher sensitivity to ε of the binding energy of cationic complexes compared to their neutral analogs. Along with this

intermolecular stretching, the θ(CH··O) bonds become slightly more linear, increasing by 2-8°. It is perhaps worthy of note that the interoxygen distance of the water dimer behaves in an opposite fashion, shortening by ~0.1 Å on going from gaseous to aqueous phase, despite its binding energy decrease. These trends are not entirely surprising as similar results were observed previously [93] for related systems.

One might expect that the solvation energy of each charged monomer should be greater than that of its complex with NMA, as the positive charge ought to be more dissipated in the larger system. And indeed, that is precisely what is found. The solvation energies reported for each system in Tables S1 and S2 show that the computed solvation energy of sulfonium $S(Me)_3^+$ is some 5-9 kcal greater than that of $S(Me)_3^+$··NMA complex, while the difference between $N(Me)_4^+$··NMA and $N(Me)_4^+$ is roughly the same. The opposite trend is observed in the neutral systems where the solvation energy of the complex exceeds that of the isolated S or N-containing monomer. And of course, the solvation energies of all charged systems are many times greater than their neutral cousins.

Distance from Center of Charge

As noted above, adding a full positive charge to the proton donor molecule greatly enhances the strength of its CH··O H-bonds. It is logical to suppose that this change is at least partly the result of a more positive bridging proton which can better interact with the O on the proton acceptor. What then might be the effect of elongating the methyl group to ethyl, propyl, etc, and thereby moving the bridging proton further from the heteroatomic center of positive charge?

M06-2X/6-31+G** calculations were performed in order to address this question. The validity of this procedure for these calculations can first be tested by comparison of the binding energies of the methyl complexes. A comparison with MP2 values is displayed in Table 1 where it may be noted that the DFT values are fairly close to MP2/aug-cc-pVDZ quantities. There is a bit of an overestimate by the former, but this overestimate is fairly uniform, roughly 1 kcal/mol.

The geometries of the ethyl and propyl parallels of the ionic methyl complexes of Fig 1 are displayed in Fig 3, along with their counterpoise-corrected binding energies, all in the gas phase. These energies are plotted against the alkyl chain length in Fig. 4, where yellow and blue curves again indicate S and N-containing complexes, respectively. The solid curves represent the structures in Fig 3 where the NMA proton acceptor binds to the terminal methyl groups in each case. Both S and N-type systems behave similarly, with the binding energy diminishing as the methyl group moves progressively further from the center of formal charge. Taking the cationic S complexes as an example, the binding energy of 22 kcal/mol for $S(CH_3)_3^+$··NMA is cut in half for the propyl analogue.

Along with a weakening of the interaction, there is a concomitant stretch of the distance between the two subunits. These distances are displayed in Table 2 for each of the three methyl groups involved in a given complex. The H-bond stretching that accompanies the lengthening of the alkyl groups is clear in this table. For example, the shortest such H-bond elongates from 2.162 to 2.254 and then to 2.420 Å as the alkyl is enlarged from methyl to ethyl to propyl in the charged S complexes; similar trends are observed in the N-containing structures.

It is not only the terminal methyl group which can engage in a CH··O H-bond, but the same is true for the methylene groups which lie closer to the heteroatom. The broken curves in Fig 4 show that when it is these CH_2 groups, those lying immediately adjacent to S or N, that form CH··O H-bonds with NMA, the drop in binding energy is much less precipitous. Put another way, if the alkyl groups are lengthened, but the O of NMA remains bonded to the CH nearest the heteroatom, there is only a small drop in binding energy. This decrease can be readily explained by the fact that the longer alkyl groups permit a greater dissipation of the overall positive charge of the cation, thereby reducing the charge on the bridging proton. Overall, then, the patterns in Fig 4 are consistent with a picture of positive charge on each cation that extends over the entire molecule, but becomes progressively smaller as one moves away from the heteroatom.

These ideas are confirmed by examination of the electrostatic potentials that surround each monomer. This potential is of course positive everywhere as the ion carries a positive charge. But there are gradations in this potential. The blue contours of Fig 5 indicate the most positive areas, and red the least positive, covering a range between 0.20 and 0.25 au. In both the S and N cases (upper and lower sections of Fig 5, respectively) as one progresses from methyl to ethyl to propyl, the terminal methyl groups become less positive, i.e. redder. Likewise, albeit more subtle, one can see a lessening of the positive potential around the H atoms that lie close to the N/S as each alkyl group grows. (The neutral molecules have a much weaker positive potential around the H atoms, peaking at around 0.08 au for $S(CH_3)_2$ and at 0.06 for $N(CH_3)_3$.) Not only the electrostatic potentials, but also the atomic charges, reflect these same patterns. The natural charges of the terminal methyl H atoms undergo a decrease as the alkyl chain elongates. For example, the average natural charge of these three H atoms is 0.28 for $N(Me)_4^+$ and drops to 0.26 in $N(Pr)_4^+$. The H atoms that lie close to the N/S also undergo a drop in positive charge, but a lesser one.

Nature of Interaction

A question that arises concerns the nature of the interaction in these charged complexes. Is it primarily a simple electrostatic interaction between the two species or is there some degree of true H-bonding, as

occurs in more classically H-bonded systems such as the water dimer? There are several vehicles to assess the nature of the interaction. For one thing, H-bonds typically involve a certain amount of charge transfer between the proton acceptor atom and the σ* antibonding orbital of the donor, as measured by NBO parameters. Table 3 reports the second-order perturbation energy E(2) for the putative CH··O H-bonds. $O_{lp}\rightarrow\sigma^*$(C-H) quantities are supplemented by transfers from the CO π bond (in parentheses). $O_{lp}\rightarrow\sigma^*$(C-H) E(2) amounts to between 0.5 and 1.7 kcal/mol for the neutral complexes, supplemented by 0.4-0.8 kcal/mol from the π(CO) bond. These quantities lie in the range of what is expected for a H-bond. They are considerably enhanced when the proton donor is charged, rising to as much as 6.7 and 1.8 kcal/mol, respectively, for the methylated systems. The former quantities refer to each individual CH··O H-bond; when summed over all three such bonds, they amount to 14-18 kcal/mol (last column of Table 3), consistent with a strong charged H-bonded complex. Note that these E(2) quantities drop as the CH donor is further removed from the heteroatom, fully consistent with the total binding energies reported above.

Decomposition of the binding energies also offers valuable clues about the nature of the interaction. Such a decomposition was carried out using the SAPT procedure, and the results are presented in Table 4. The electrostatic is the largest component for the ionic complexes in the last two columns, followed by induction and dispersion which make comparable contributions to one another. This pattern is consistent with what one would expect for H-bonds. The neutral complexes have a much reduced electrostatic component, although the dispersion energy is comparable to that of the ionic systems. The larger DISP as compared to ES is not a feature typically seen in H-bonds, although it does occur on occasion.

Yet another tool used to distinguish H-bonds concerns the electron density. More specifically, there is a characteristic pattern that occurs within the shifts of electron density when a H-bond is formed. These shifts are illustrated in Fig 6 where gains of density are indicated by blue contours and losses by red. In all complexes, there is a red region of density loss surrounding each bridging proton, as well as a blue region of gain in the vicinity of the proton-accepting O atom of NMA. This pattern reproduces a typical fingerprint of H-bond formation so supports its characterization as such. Further confirmation arises from the observation that these same patterns become more intense as the binding energy rises, as in the progression $S(Me)_2 < S(Pr)_3^+ < S(Et)_3^+ < S(Me)_3^+$.

Whereas the formation of conventional H-bonds, e.g. OH··O, induces a stretching of the O-H bond in the proton donor molecule, the situation with CH··O analogues has been found to be less predictable. While there is a trend for sp-hybridized CH bonds, as in HCCH, to stretch just like their OH counterparts, those that are engaged in sp^3 hybridization tend [32] to contract, although this is not a hard and fast rule. The geometric changes occurring within the proton donor molecules here obey an interesting pattern. The

bridging CH bond of the terminal methyl groups of the sulfonium SR_3^+ cation stretches when R=Me or Et, but undergoes a contraction for R=Pr; the same is true for the N-containing molecules. On the other hand, when the bridging proton is associated with a methylene group that is immediately adjacent to the S/N heteroatom, the CH bond undergoes a small contraction, less than 3 mÅ.

A useful experimental tool for identifying H-bonds resides in NMR spectroscopy, as the bridging proton typically shifts downfield [94, 95] by several ppm. Prior work has shown that CH··O H-bonds conform to this trend [96-98], albeit generally exhibiting a smaller shift which comports with the weaker nature of this H-bond. In order therefore to add to our pallet of H-bond identification tools, the NMR chemical shieldings were computed for the various protons in each of the systems described above. The changes in the shielding, as compared to the isolated monomers, are reported in the first two columns of data in Table 5 where negative values correspond to a deshielding and downfield shift. As the geometries reflect a trifurcated arrangement, with very similar CH··O H-bond energies, it is not surprising to see very similar shifts for the three corresponding protons. Consequently, the values listed in Table 5 refer to the average changes of all three bridging protons. (Nonbridging protons exhibit much smaller changes, and in the upfield direction.)

Inspection of Table 5 quickly reveals that the downfield shifts are roughly proportional to the H-bond energies. Taking the S series as an example, the shift for neutral thioether $S(Me)_2$ is less than 1 ppm, but this quantity enlarges to 2.23 ppm for the cationic $S(Me)_3^+$. Following down the first column of Table 5, it is clear that as the terminal methyl group moves further from the S atom, the shift lowers eventually down to 1.15 ppm for the tripropyl species. The next column of Table 5 refers to those complexes wherein the NMA acceptor binds not to the terminal methyl group, but rather to the methylene group adjacent to S. Just as in the case of the binding energy, the downfield shift is lowered much more slowly as the alkyl chain grows, remaining above 2 ppm. Very similar trends are observed for the N series. It may be concluded that the NMR chemical shifts fully support the characterization of these interactions as full bodied H-bonds.

Rapid rotations of methyl groups frequently make it difficult to experimentally separate the NMR signals of the bridging proton of a given methyl group from the H atoms that are not so involved. What is frequently observed instead is an average of all three of these signals. Therefore as a guide to experimentalists, the third column of Table 5 reports the average change in the chemical shielding of all protons of the terminal H-bonded methyl groups, both H-bonded and non-H-bonded. Due to the upfield shift of the latter, these averages are much smaller in magnitude than those in the first column, but are

downfield nonetheless. As a rule of thumb, the downfield shift is less than -0.1 ppm for the neutral complexes, but lies in the range between -0.3 and -0.5 for the ionic H-bonds.

With specific respect to methyl rotations, each methyl group is staggered with respect to its neighbors in its optimal orientation. Rotation of a single methyl must cross a barrier which involves an eclipsed structure. These barriers are calculated in the methyl derivatives to vary from 2.2-2.6 kcal/mol for the thioethers and 4.8-5.0 kcal/mol for the amines When complexed with NMA, the barriers increase a small amount, between 0.1 and 0.9 kcal/mol, presumably due to the disruption of one of the CH··O H-bonds.

Other Geometries of H-bonds

As indicated above, the most stable configuration of each dimer involves a trifurcated H-bond, in the sense that the NMA O atom engages in a H-bond simultaneously with three CH bonds, each on a different alkyl chain. The question that comes to mind is how much the energy might suffer if the trifurcation involves the three H atoms on a single methyl group. In order to answer this question, a set of restricted geometry optimizations were carried out wherein the θ(XC··O) angle (X=S,N, or C) was held equal to 180°. Counterpoise-corrected binding energies are plotted against the length of the alkyl chain in Fig 7 as broken curves where yellow and blue lines again represent S^+ and N^+ complexes respectively. It is first clear that these binding energies diminish as the chain elongates and the terminal methyl group is drawn further from the heteroatomic center of positive charge, just as was noted earlier. The very near coincidence of the yellow and blue curves in Fig 7 indicates there is little difference imparted by the nature of this heteroatom. But perhaps most importantly, the binding energies in Fig 7 are considerably lower than those in Fig 4 so that one may conclude that trifurcation with three separate alkyl chains is preferable to trifurcation with a single methyl group. For example, the trifurcated complexes for the $N(CH_3)_4^+$ and $S(CH_3)_3^+$ cations in Fig 4 are bound by 20.3 and 22.2 kcal/mol respectively, considerably larger than the 14.5 kcal/mol when the O is allowed to interact with a single methyl group of either cation.

Part of the explanation of this weaker interaction is likely due to greater strain of the H-bonds. The θ(CH··O) angles lie in the 84-91° range for the single methyl group, but this range extends to 125-151° when three separate methyl groups interact with the proton acceptor. NBO analysis confirms that this angular factor is important. The small θ(CH··O) angles hinder the transfer of charge from the O lone pair to a CH σ* antibond. Instead, what charge transfer there is goes from the O lone pair to the σ* antibonding orbital of the X-C bond (X=S,N,C). And it should be emphasized the E(2) is rather small in any case, between 0.7 and 3.1 kcal/mol. Other evidence for the weakness of these H-bonds arises from the calculated NMR spectrum. As reported in the penultimate column of Table 5, the three bridging protons shift downfield by only 0.4 - 0.8 ppm, considerably less than the values listed in the preceding columns of

Table 5 when three separate methyl groups are involved in the trifurcated arrangement. Finally, this trifurcated interaction with a single methyl group results in small contractions of the three C-H bonds, but only by about 1 mÅ, and this bond shortening is attenuated as the alkyl chain is elongated from methyl to butyl.

Another possibility which is worthy of examination involves a single, linear CH··O H-bond. Since there is no minimum on the surface that corresponds to such a structure, a restriction of θ(CH··O)=180° was introduced into the geometry optimization, after placing the NMA O atom proximate to a terminal methyl group. The counterpoise-corrected binding energies of these complexes are displayed as the solid curves in Fig 7, where again one sees a diminishing trend as the alkyl chain elongates. Note that these solid curves are slightly higher than the broken curves, suggesting that a single linear CH··O H-bond is energetically superior to a trifurcated arrangement with one methyl group. In other words, a proton acceptor prefers to approach a methyl group along a C-H axis as compared to the tetrahedron face. But even these linear CH··O H-bonds are inferior to the trifurcated arrangements of Fig 4 which involve three different alkyl chains. As a secondary issue, the formation of the linear CH··O H-bonds results in a C-H stretch. In the case of the S cations, this elongation varies from a minimum of 0.4 mÅ for the terminal methyl of a butyl chain to 4.5 mÅ for a methyl group. The stretch is consonant with charge transfer into the CH σ* antibond, which is largest for the methyl group where E(2)=13.7 kcal/mol, and decreases monotonically as the alkyl chain elongates, to a minimum of 4.3 kcal/mol for the butyl chain. The strength of this single H-bond is further underscored by the NMR signal of the bridging proton, which the last column of Table 5 shows to shift downfield by 2.5 - 3.5 ppm, a somewhat greater amount than in the case of the three separate, bent H-bonds of the preceding columns of Table 5. As in the earlier bonding situations, the shift is roughly proportional to the binding energy, diminishing as the alkyl chain is elongated and the bridging proton is removed further from the S/N center of charge.

There were additional minima located in the potential energy surfaces that offer further refinements in terms of geometric preferences. For example, as one might expect two H-bonds are inferior to three, when all proton donors are terminal methyl groups. Similarly, a complex containing two H-bonds to methylene protons is of course more weakly bound than one which makes use of three such methylenes. On the other hand, these same two H-bonds that involve groups close to the S/N center of positive charge are superior to three CH··O bonds to terminal methyl groups, further from this center.

SUMMARY AND DISCUSSION

The alkylated thioethers and amines engage in CH··O H-bonding to the NMA proton acceptor, with binding energies of 2-5 kcal/mol. The addition of a positive charge to the proton donor molecule

magnifies the interaction by a factor of 5-9, such that sulfonium $S(Me)_3^+$ is bound to NMA by more than 20 kcal/mol. In all cases, the proton acceptor atom prefers interacting with as many CH groups as possible, i.e. multiple bent CH··O H-bonds are more favorable than a single linear one. There is also an energetic preference for the O to interact with H atoms on separate alkyl groups, as compared to several H atoms on the same R. H atoms that lie closer to the central atom with its formal charge make the strongest H-bonds. The binding energy drops much more precipitously with alkyl chain length if the O is able to interact only with the terminal methyl H atoms, furthest from the central atom. This phenomenon may be explained on the basis of an attenuating positive electrostatic potential as one moves further from the S or N center of positive charge. The H-bonds formed by CH donors in species with a central S atom are slightly stronger than in the case of the amines. With regard to environment, the strengths of the CH··O H-bonds are reduced as the solvent in which the systems are immersed becomes more polarizable. Nonetheless, the ionic $^+$CH··O H-bonds remain stronger than neutral OH··O analogues, even in aqueous solution.

The CH··O interactions have all the hallmarks of true H-bonds. The shifts of electron density that accompany the formation of the dimers fit the usual fingerprint pattern of H-bonds. NBO analysis reveals a transfer of charge into the CH σ* antibonding orbital, and the magnitude of the corresponding second order energies are proportional to the overall binding energies. NMR chemical shifts of the bridging protons reflect the deshielding that is another marker of H-bonds, and this shift is roughly proportional to binding energy. SAPT decomposition of the total interaction energy shows the dominant term to be electrostatic, but very substantial contributions are made by induction and dispersion as well. The change in the C-H bond length caused by H-bond formation is not uniform. Whereas this bond undergoes a stretch for the more strongly bound complexes, this trend reverses as the H-bond weakens. This pattern is not unlike what has been seen over the years for other CH··O H-bonds, some of which lengthen while others contract.

The results described here agree well with earlier work in the recent literature on related systems. Our binding energy of $N(CH_3)_4^+$ compares nicely with an earlier computation where this cation was paired with water for a binding energy of 9.7 kcal/mol at the MP2/6-311+G** level [66]. When other authors [67] interacted $HN(CH_3)_3^+$ with an ester O, their optimized structure contained a trifurcated H-bond with three separate methyl groups like the ones found here, and with a binding energy of 12.9 kcal/mol with a 6-311++G** basis set. When this system was immersed in a dielectric medium, the binding energy suffered diminution, and became repulsive for $\varepsilon > 8$. Other $^+$CH··O H-bonds were also found to drop in binding energy as dielectric constant was raised [70], in this case with methylpyridinium as proton donor. And a very

recent work [99] agreed that a single linear $^{+}$CH···O H-bond is energetically superior to a bifurcated arrangement when both H atoms are bonded to the same C.

There has been some question as to whether the interaction between an amine and proton acceptor such as NMA is strengthened by the charge or by the number of methyl groups bound to the central N atom. That is, what is the difference between adding a charge via a fourth methyl group to form $N(CH_3)_4^+$ as was done here, as compared to forming the cation via addition of a proton, as in $HN(CH_3)_3^+$ as might occur in low-pH solution? A full geometry optimization via the MP2/aug-cc-pVDZ of the complex between NMA and $HN(CH_3)_3^+$ was therefore performed. The counterpoise-corrected binding energy was computed to be 19.5 kcal/mol, 0.7 kcal/mol stronger than that of the tetramethylammonium complex of Fig 1d. The details of the two geometries are nearly identical, with R(CH··O)=2.2 Å in either case, and with θ(CH··O) angles within 1° of one another. The very small energetic advantage of the $HN(CH_3)_3^+$ complex may be attributed to a slightly greater concentration of positive charge on the three remaining methyl groups.

It would appear then that $^{+}$CH··O H-bonds can be quite strong, with binding energies as high as 20 kcal/mol. These bonds exceed the strength of the typical NH··O=C H-bonds that provide the organizing force for such common protein structures as α-helix or β-sheet. While attenuated somewhat within the context of a polarizable medium, they nonetheless retain their greater strength when compared to neutral H-bonds. As such, these H-bonds can exert a strong influence on enzyme activity or in binding of substrates.

The calculations reveal a greater depth about the specifics of the mode of binding. When a substrate of the type SR_3^+ is placed within a protein interior, there will be a strong tendency for its CH groups to engage in CH··O H-bonds with neighboring residues. If only a single proton acceptor is nearby, the overall preference will bring that acceptor as close as possible to the central S atom, and for three separate R chains to all participate in the trifurcated H-bonding. The interaction will weaken if the acceptor is forced by steric constraints to interact with CH groups that lie further from S, e.g. the terminal methyl groups. If other constraints permit H-bonding of the acceptor to only one methyl, a single CH··O is favored over three bent H-bonds to that same methyl group. But the latter issues notwithstanding, it is emphasized that even with some of these weakening factors in play, $^{+}$CH··O H-bonds are strong ones, surpassing neutral H-bonds, even those involving the electronegative O and N atoms as proton donors.

ACKNOWLEDGMENTS

This work was supported by the National Science Foundation (CHE-1026826). Computer, storage and other resources from the Division of Research Computing in the Office of Research and Graduate Studies at Utah State University are gratefully acknowledged.

Supporting Information Available:

The full list of authors of refs 6, 73, and 89 is followed by Tables S1 and S2. This information is available free of charge via the Internet at http://pubs.acs.org.

REFERENCES

1. Gilli, G.; Gilli, P., *The Nature of the Hydrogen Bond*; Oxford University Press: Oxford, UK, 2009.
2. Scheiner, S., *Hydrogen Bonding: A Theoretical Perspective*; Oxford University Press: New York, 1997.
3. *Hydrogen Bonding - New Insights;* Grabowski, S. J., Ed.; Springer: Dordrecht, 2006.
4. *The Hydrogen Bond. Recent Developments in Theory and Experiments;* Schuster, P.; Zundel, G.; Sandorfy, C., Ed.; North-Holland Publishing Co.: Amsterdam, 1976.
5. Desiraju, G. R.; Steiner, T., *The Weak Hydrogen Bond in Structural Chemistry and Biology*; Oxford: New York, 1999.
6. Arunan, E.; Desiraju, G. R.; Klein, R. A.; Sadlej, J.; Scheiner, S.; Alkorta, I.; Clary, D. C.; Crabtree, R. H.; Dannenberg, J. J.; Hobza, P. et al. Definition of the Hydrogen Bond. *Pure Appl. Chem.* **2011,** *83*, 1637-1641.
7. Oliveira, B. G. d. Structure, energy, vibrational spectrum, and Bader's analysis of π···H hydrogen bonds and $H^{-\delta}\cdots H^{+\delta}$ dihydrogen bonds. *Phys. Chem. Chem. Phys.* **2013,** *15*, 37-79.
8. Kar, T.; Scheiner, S. Comparison between hydrogen and dihydrogen bonds among H_3BNH_3, H_2BNH_2, and NH_3. *J. Chem. Phys.* **2003,** *119*, 1473-1482.
9. Singh, P. C.; Patwari, G. N. The C–H···H–B dihydrogen bonded borane-trimethylamine dimer: A computational study. *Chem. Phys. Lett.* **2006,** *419*, 265-268.
10. Belkova, N. V.; Shubina, E. S.; Epstein, L. M. Diverse world of unconventional hydrogen bonds. *Acc. Chem. Res.* **2005,** *38*, 624-631.
11. Solimannejad, M.; Scheiner, S. Theoretical Investigation of the dihydrogen bond linking MH_2 with HCCRgF (M=Zn,Cd; Rg=Ar,Kr). *J. Phys. Chem. A* **2005,** *109*, 11933-11935.
12. Saggu, M.; Levinson, N. M.; Boxer, S. G. Experimental quantification of electrostatics in X–H···π hydrogen bonds. *J. Am. Chem. Soc.* **2012,** *134*, 18986-18997.
13. Nishio, M. The CH/π hydrogen bond in chemistry. Conformation, supramolecules, optical resolution and interactions involving carbohydrates. *Phys. Chem. Chem. Phys.* **2011,** *13*, 13873-13900.
14. Takahashi, O.; Kohno, Y.; Nishio, M. Relevance of weak hydrogen bonds in the conformation of organic compounds and bioconjugates: Evidence from recent experimental eata and high-level ab initio MO calculations. *Chem. Rev.* **2010,** *110*, 6049-6076.
15. Nakanaga, T.; Buchhold, K.; Ito, F. Investigation of the NH-π hydrogen bond interaction in the aniline-alkene (C_2H_4, C_3H_6, C_4H_8) cluster cations by infrared depletion spectroscopy. *Chem. Phys.* **2003,** *288*, 69-76.
16. Bhattacherjee, A.; Matsuda, Y.; Fujii, A.; Wategaonkar, S. The intermolecular S-H···Y (Y=S,O) hydrogen bond in the H_2S dimer and the H_2S–MeOH complex. *ChemPhysChem.* **2013,** *14*, 905-914.
17. Grzechnik, K.; Rutkowski, K.; Mielke, Z. The S–H···N versus O–H···N hydrogen bonding in the ammonia complexes with CH_3OH and CH_3SH. *J. Mol. Struct.* **2012,** *1009*, 96-102.
18. Biswal, H. S.; Wategaonkar, S. Sulfur, not too far behind O, N, and C: SH···π hydrogen bond. *J. Phys. Chem. A* **2009,** *113*, 12774-12782.
19. Allerhand, A.; Schleyer, P. v. R. A survey of C-H groups as proton donors in hydrogen bonding. *J. Am. Chem. Soc.* **1963,** *85*, 1715-1723.
20. Krimm, S.; Kuroiwa, K. Low temperature infrared spectra of polyglycines and C—H … O=C hydrogen bonding in polyglycine II. *Biopolymers* **1968,** *6*, 401-407.
21. Gu, Y.; Kar, T.; Scheiner, S. Comparison of the CH···N and CH···O interactions involving substituted alkanes. *J. Mol. Struct.* **2000,** *552*, 17-31.

22. Howard, N. W.; Legon, A. C. Pulsed-nozzle, Fourier-transform microwave spectroscopy of the methyl cyanide-acetylene dimer. *J. Chem. Phys.* **1986,** *85*, 6898-6904.
23. Kryachko, E.; Scheiner, S. CH··F hydrogen bonds. Dimers of fluoromethanes. *J. Phys. Chem. A* **2004,** *108*, 2527-2535.
24. Scheiner, S. Contributions of NH··O and CH··O H-bonds to the stability of β-sheets in proteins. *J. Phys. Chem. B* **2006,** *110*, 18670-18679.
25. van der Veken, B. J.; Delanoye, S. N.; Michielsen, B.; Herrebout, W. A. A cryospectroscopic study of the blue-shifting C–H¨O bonded complexes of pentafluoroethane with dimethyl ether-d_6, acetone-d_6 and oxirane-d_4. *J. Mol. Struct.* **2010,** *976*, 97-104.
26. You, L.-Y.; Chen, S.-G.; Zhao, X.; Liu, Y.; Lan, W.-X.; Zhang, Y.; Lu, H.-J.; Cao, C.-Y.; Li, Z.-T. C-H¨O hydrogen bonding induced triazole foldamers: Efficient halogen bonding receptors for organohalogens. *Angew. Chem. Int. Ed.* **2012,** *51*, 1657-1661.
27. Scheiner, S., The CH--O Hydrogen Bond. A Historical Account. In *Theory and Applications of Computational Chemistry: The First 40 Years*, ed.; Dykstra, C. E.; Frenking, G.; Kim, K. S.; Scuseria, G. E., 'Ed.'^'Eds.' Elsevier: Amsterdam, 2005; p^pp 831-857.
28. Scheiner, S. Theoretical analysis of the contributions made by CH¨O H-bonds to protein structure. *Curr. Org. Chem.* **2010,** *14*, 106-128.
29. Barnes, A. J.; Beech, T. R. The vibrational spectrum of the dimethyl ether-water complex. *Chem. Phys. Lett.* **1983,** *94*, 568-570.
30. Scheiner, S.; Kar, T. Spectroscopic and structural signature of the CH--O H-bond. *J. Phys. Chem. A* **2008,** *112*, 11854-11860.
31. Zierkiewicz, W.; Czarnik-Matusewicz, B.; Michalska, D. Blue shifts and unusual intensity changes in the infrared spectra of the enflurane···acetone complexes: Spectroscopic and theoretical studies. *J. Phys. Chem. A* **2011,** *115*, 11362-11368.
32. Scheiner, S.; Grabowski, S. J.; Kar, T. Influence of hybridization and substitution upon the properties of the CH··O hydrogen bond. *J. Phys. Chem. A* **2001,** *105*, 10607-10612.
33. Ford, T. A.; Glasser, L. Ab initio calculations of the structural, energetic and vibrational properties of some hydrogen bonded and van der Waals dimers. Part 3. The formaldehyde dimer. *J. Mol. Struct. (Theochem)* **1997,** *398-399*, 381-394.
34. Cubero, E.; Orozco, M.; Hobza, P.; Luque, F. J. Hydrogen bond versus anti-hydrogen bond: A comparative analysis based on the electron density topology. *J. Phys. Chem. A* **1999,** *103*, 6394-6401.
35. Grabowski, S. J. Red- and blue-shifted hydrogen bonds: The Bent rule from quantum theory of atoms in molecules perspective. *J. Phys. Chem. A* **2011,** *115*, 12789-12799.
36. Michielsen, B.; Dom, J. J. J.; van der Veken, B. J.; Hesse, S.; Xue, Z.; Suhm, M. A.; Herrebout, W. A. The complexes of halothane with benzene: the temperature dependent direction of the complexation shift of the aliphatic C–H stretching. *Phys. Chem. Chem. Phys.* **2010,** *12*, 14034-14044.
37. Deakyne, C. A.; Meot-Ner, M. Ionic hydrogen bonds in bioenergetics. 4. Interaction energies of acetylcholine with aromatic and polar molecules. *J. Am. Chem. Soc.* **1999,** *121*, 1546-1557.
38. Bojin, M. D.; Tantillo, D. J. Nonclassical carbocations as C-H hydrogen bond donors. *J. Phys. Chem. A* **2006,** *110*, 4810-4816.
39. Cybulski, S. M.; Scheiner, S. Comparison of Morokuma and perturbation theory approaches to decomposition of interaction energy. $(NH_4)^+$...NH_3. *Chem. Phys. Lett.* **1990,** *166*, 57-64.
40. Shishkin, O. V.; Palamarchuk, G. V.; Gorb, L.; Leszczynski, J. Opposite charges assisted extra strong C–H¨O hydrogen bond in protonated 2'-deoxyadenosine monophosphate. *Chem. Phys. Lett.* **2008,** *452*, 198-205.

41. Meot-Ner, M. The ionic hydrogen bond and ion solvation. 1. $NH^{+}\cdots O$, $NH^{+}\cdots N$, and $OH^{+}\cdots O$ bonds. Correlations with proton affinity. Deviations due to structural effects. *J. Am. Chem. Soc.* **1984,** *106*, 1257-1264.
42. Scheiner, S.; Redfern, P.; Szczesniak, M. M. Effects of external ions on the energetics of proton transfers across hydrogen bonds. *J. Phys. Chem.* **1985,** *89*, 262-266.
43. Meot-Ner, M.; Sieck, L. W. The ionic hydrogen bond and ion solvation. 5. $OH\cdots O^{-}$ bonds. Gas phase solvation and clustering of alkoxide and carboxylate anions. *J. Am. Chem. Soc.* **1986,** *108*, 7525-7529.
44. Meot-Ner, M. Comparative stabilities of cationic and anionic hydrogen-bonded networks. Mixed clusters of water-methanol. *J. Am. Chem. Soc.* **1986,** *108*, 6189-6197.
45. Szczesniak, M. M.; Scheiner, S. Møller-Plesset treatment of electron correlation in $(HOHOH)^{-}$. *J. Chem. Phys.* **1982,** *77*, 4586-4593.
46. Paul, G. J. C.; Kebarle, P. Thermodynamics of the association reactions of $OH^{-} + H_2O = HOHOH^{-}$ and $CH_3O^{-} + CH_3OH = CH_3OHOCH_3^{-}$ in the gas phase. *J. Phys. Chem.* **1990,** *94*, 5184-5189.
47. Gronert, S. Theoretical studies of proton transfers. 1. The potential energy surfaces of the identity reactions of the first- and second-row non-metal hydrides with their conjugate bases. *J. Am. Chem. Soc.* **1993,** *115*, 10258-10266.
48. Berger, I.; Egli, M.; Rich, A. Inter-strand C-H···O hydrogen bonds stabilizing four-stranded intercalated molecules: Stereoelectronic effects of O4' in cytosine-rich DNA. *Proc. Nat. Acad. Sci., USA* **1996,** *93*, 12116-12121.
49. Mallinson, P. R.; Wozniak, K.; Smith, G. T.; McCormack, K. L. A charge density analysis of cationic and anionic hydrogen bonds in a "proton sponge" complex. *J. Am. Chem. Soc.* **1997,** *119*, 11502-11509.
50. Chabinyc, M. L.; Brauman, J. I. Acidity, basicity, and the stability of hydrogen bonds: Complexes of $RO^{-} + HCF_3$. *J. Am. Chem. Soc.* **1998,** *120*, 10863-10870.
51. Felemez, M.; Bernard, P.; Schlewer, G.; Spiess, B. Inframolecular protonation process of *myo*-inositol 1,4,5-tris(phosphate) and related compounds: Dynamics of the intramolecular interactions and evidence of C-H···O hydrogen bonding. *J. Am. Chem. Soc.* **2000,** *122*, 3156-3165.
52. Kryachko, E. S.; Zeegers-Huyskens, T. Theoretical study of the $CH\cdots X^{-}$ interaction of fluoromethanes and chloromethanes with fluoride, chloride, and hydroxide anions. *J. Phys. Chem. A* **2002,** *106*, 6832-6838.
53. Wang, X.-B.; Woo, H.-K.; Kiran, B.; Wang, L.-S. Observation of weak C-H···O hydrogen bonding to unactivated alkanes. *Angew. Chem., Int. Ed. Engl.* **2005,** *44*, 4968-4972.
54. Li, Y.; Flood, A. H. Pure C-H hydrogen bonding to chloride ions: A preorganized and rigid macrocyclic receptor. *Angew. Chem., Int. Ed. Engl.* **2008,** *47*, 2649-2652.
55. Pedzisa, L.; Hay, B. P. Aliphatic C-H···anion hydrogen bonds: Weak contacts or strong interactions? *J. Org. Chem.* **2009,** *74*, 2554-2560.
56. Yang, H.; Wong, M. W. Oxyanion hole stabilization by C-H···O interaction in a transition state-A three-point interaction model for cinchona alkaloid-catalyzed asymmetric methanolysis of meso-cyclic anhydrides. *J. Am. Chem. Soc.* **2013,** *135*, 5808-5818.
57. Tatko, C. D.; Waters, M. L. Comparison of C-H···π and jydrophobic interactions in a β-hairpin peptide: Impact on stability and specificity. *J. Am. Chem. Soc.* **2004,** *126*, 2028 - 2034.
58. Schmiedekamp, A.; Nanda, V. Metal-activated histidine carbon donor hydrogen bonds contribute to metalloprotein folding and function. *J. Inorg. Biochem.* **2009,** *103*, 1054-1060.
59. Sukumar, N.; Mathews, F. S.; Langan, P.; Davidson, V. L. A joint x-ray and neutron study on amicyanin reveals the role of protein dynamics in electron transfer. *Proc. Nat. Acad. Sci., USA* **2010,** *107*, 6817-6822.

60. Couture, J.-F.; Hauk, G.; Thompson, M. J.; Blackburn, G. M.; Trievel, R. C. Catalytic roles for carbon-oxygen hydrogen bonding in SET domaine lysine methyltransferases. *J. Biol. Chem.* **2006,** *281*, 19280-19287.
61. Couture, J.-F.; Collazo, E.; Ortiz-Tello, P. A.; Brunzelle, J. S.; Trievel, R. C. Specificity and mechanism of JMJD2A, a trimethyllysine-specific histone demethylase. *Nat. Struct. Mol. Biol.* **2007,** *14*, 689-695.
62. Couture, J.-F.; Dirk, L. M. A.; Brunzelle, J. S.; Houtz, R. L.; Trievel, R. C. Structural origins for the product specificity of SET domain protein methyltransferases. *Proc. Nat. Acad. Sci., USA* **2008,** *105*, 20659-20664.
63. Del Rizzo, P. A.; Couture, J.-F.; Dirk, L. M. A.; Strunk, B. S.; Roiko, M. S.; Brunzelle, J. S.; Houtz, R. L.; Trievel, R. C. SET7/9 catalytic mutants reveal the role of active site water molecules in lysine multiple methylation. *J. Biol. Chem.* **2010,** *285*, 31849-31858.
64. Horowitz, S.; Yessleman, J. D.; Al-Hashimi, H. M.; Trievel, R. C. Direct evidence for methyl group coordination by carbon-oxygen hydrogen bonds in the lysine methyltransferase SET7/9. *J. Biol. Chem.* **2011,** *286*, 18658-18663.
65. Sreerama, N.; Vishveshwara, S. An ab initio study of $(C\text{-}H^{\cdots}X)^{+}$ hydrogen bonds including biological systems. *J. Mol. Struct. (Theochem)* **1985,** *133*, 139-146.
66. Kim, K. S.; Lee, J. Y.; Lee, S. J.; Ha, T.-K.; Kim, D. H. On binding forces between aromatic ring and quaternary ammonium compound. *J. Am. Chem. Soc.* **1994,** *116*, 7399-7400.
67. Cannizzaro, C. E.; Houk, K. N. Magnitude and chemical consequences of R_3N^{+}-C-H$^{\cdots}$O=C hydrogen bonding. *J. Am. Chem. Soc.* **2002,** *124*, 7163-7169.
68. Scheiner, S.; Kar, T.; Gu, Y. Strength of the $C^{\alpha}H^{\cdots}O$ hydrogen bond of amino acid residues. *J. Biol. Chem.* **2001,** *276*, 9832-9837.
69. Kryachko, E. S.; Nguyen, M. T. Low energy barrier proton transfer in protonated benzene-water complex. *J. Phys. Chem. A* **2001,** *105*, 153-155.
70. Raymo, F. M.; Bartberger, M. D.; Houk, K. N.; Stoddart, J. F. The magnitude of [C-H$^{\cdots}$O] hydrogen bonding in molecular and supramolecular assemblies. *J. Am. Chem. Soc.* **2001,** *123*, 9264-9267.
71. Scheiner, S.; Kar, T.; Pattanayak, J. Comparison of various types of hydrogen bonds involving aromatic amino acids. *J. Am. Chem. Soc.* **2002,** *124*, 13257-13264.
72. Chang, H.-C.; Lee, K. M.; Jiang, J.-C.; Lin, M.-S.; Chen, J.-S.; Lin, I. J. B.; Lin, S. H. Charge-enhanced C–HO interactions of a self-assembled triple helical spine probed by high-pressure. *J. Chem. Phys.* **2002,** *117*, 1723-1728.
73. Frisch, M. J.; Trucks, G. W.; Schlegel, H. B.; Scuseria, G. E.; Robb, M. A.; Cheeseman, J. R.; Scalmani, G.; Barone, V.; Mennucci, B.; Petersson, G. A. et al. *Gaussian 09*, Revision B.01; Wallingford, CT, 2009.
74. Singh, P. C. C–H$^{\cdots}$O/N hydrogen bonded complexes of FKrCCH are stronger than FCCH complexes: Effect of rare gas insertion. *Chem. Phys. Lett.* **2011,** *515*, 206-209.
75. Li, H.; Lu, Y.; Liu, Y.; Zhu, X.; Liu, H.; Zhu, W. Interplay between halogen bonds and π–π stacking interactions: CSD search and theoretical study. *Phys. Chem. Chem. Phys.* **2012,** *14*, 9948-9955.
76. Riley, K. E.; Murray, J. S.; Fanfrlík, J.; Rezác, J.; Solá, R. J.; Concha, M. C.; Ramos, F. M.; Politzer, P. Halogen bond tunability I: the effects of aromatic fluorine substitution on the strengths of halogen-bonding interactions involving chlorine, bromine, and iodine. *J. Mol. Model.* **2011,** *17*, 3309-3318.
77. Hauchecorne, D.; Nagels, N.; van der Veken, B. J.; Herrebout, W. A. C–X$^{\cdots}$π halogen and C–H$^{\cdots}$π hydrogen bonding: Interactions of CF_3X (X = Cl, Br, I or H) with ethene and propene. *Phys. Chem. Chem. Phys.* **2012,** *14*, 681-690.

78. Scheiner, S. Effects of substituents upon the P···N noncovalent interaction: The limits of its strength. *J. Phys. Chem. A* **2011,** *115*, 11202-11209.
79. Munusamy, E.; Sedlak, R.; Hobza, P. On the nature of the stabilization of benzene···dihalogen and benzene···dinitrogen complexes: CCSD(T)/CBS and DFT-SAPT calculations. *ChemPhysChem.* **2011,** *12*, 3253-3261.
80. Zhao, Y.; Truhlar, D. G. The M06 suite of density functionals for main group thermochemistry, thermochemical kinetics, noncovalent interactions, excited states, and transition elements: two new functionals and systematic testing of four M06-class functionals and 12 other functionals. *Theor. Chem. Acc.* **2008,** *120*, 215-241.
81. Vincent, M. A.; Hillier, I. H. The structure and interaction energies of the weak complexes of $CHClF_2$ and CHF_3 with HCCH: A test of density functional theory methods. *Phys. Chem. Chem. Phys.* **2011,** *13*, 4388-4392.
82. Biller, M. J.; Mecozzi, S. A high level computational study of the CH_4/CF_4 dimer: How does it compare with the CH_4/CH_4 and CF_4/CF_4 dimers? *Mol. Phys.* **2012,** *110*, 377-387.
83. Majumder, M.; Mishra, B. K.; Sathyamurthy, N. CH···π and π···π interaction in benzene-acetylene clusters. *Chem. Phys.* **2013,** *557*, 59-65.
84. Karthikeyan, S.; Ramanathan, V.; Mishra, B. K. Influence of the substituents on the CH···π interaction: Benzene–methane complex. *J. Phys. Chem. A* **2013,** *117*, 6687-6694.
85. Boys, S. F.; Bernardi, F. The calculation of small molecular interactions by the differences of separate total energies. Some procedures with reduced errors. *Mol. Phys.* **1970,** *19*, 553-566.
86. Reed, A. E.; Weinhold, F.; Curtiss, L. A.; Pochatko, D. J. Natural bond orbital analysis of molecular interactions: Theoretical studies of binary complexes of HF, H_2O, NH_3, N_2, O_2, F_2, CO and CO_2 with HF, H_2O, and NH_3. *J. Chem. Phys.* **1986,** *84*, 5687-5705.
87. Reed, A. E.; Curtiss, L. A.; Weinhold, F. Intermolecular interactions from a natural bond orbital, donor-acceptor viewpoint. *Chem. Rev.* **1988,** *88*, 899-926.
88. Moszynski, R.; Wormer, P. E. S.; Jeziorski, B.; van der Avoird, A. Symmetry-adapted perturbation theory of nonadditive three-body interactions in van der Waals molecules. I. General theory. *J. Chem. Phys.* **1995,** *103*, 8058-8074.
89. Werner, H.-J.; Knowles, P. J.; Manby, F. R.; Schütz, M.; P. Celani; Knizia, G.; Korona, T.; Lindh, R.; Mitrushenkov, A.; Rauhut, G. et al. *MOLPRO*, Version 2006; 2010.
90. Barone, V.; Cossi, M. Quantum calculation of molecular energies and energy gradients in solution by a conductor solvent model. *J. Phys. Chem. A* **1998,** *102*, (11), 1995-2001.
91. Ditchfield, R. Self-consistent perturbation theory of diamagnetism. I. A gauge-invariant LCAO method for N.M.R. chemical shifts. *Mol. Phys.* **1974,** *27*, 789-807.
92. Wolinski, K.; Hilton, J. F.; Pulay, P. Efficient implementationi of the gauge-independent atomic orbital method for NMR chemical shift calculations. *J. Am. Chem. Soc.* **1990,** *112*, 8251-8260.
93. Scheiner, S.; Kar, T. Effect of solvent upon CH··O hydrogen bonds with implications for protein folding. *J. Phys. Chem. B* **2005,** *109*, 3681-3689.
94. Ando, S.; Ando, I.; Shoji, A.; Ozaki, T. Intermolecular hydrogen-bonding effect on carbon-13 NMR chemical shifts of glycine residue carbonyl carbons of peptides in the solid state. *J. Am. Chem. Soc.* **1988,** *110*, (11), 3380-3386.
95. Hibbert, F.; Emsley, J. Hydrogen bonding and chemical reactivity. *Adv. Phys. Org. Chem.* **1990,** *26*, 255-379.
96. Mizuno, K.; Ochi, T.; Shindo, Y. Hydrophobic hydration of acetone probed by nuclear magnetic resonance and infrared: Evidence for the interaction C-H···OH_2. *J. Chem. Phys.* **1998,** *109*, 9502-9507.
97. Afonin, A. V.; Vashchenko, A. V.; Takagi, T.; Kimura, A.; Fujiwara, H. Specific intramolecular interactions C-H···N in heteroaryl vinyl ethers and heteroaryl vinyl sulfides studied by ^{1}H, ^{13}C, and

^{15}N NMR spectroscopies and by ab initio calculations on molecular structures as well as on nuclear shieldings. *Can. J. Chem.* **1999,** *77*, 416-424.
98. Scheiner, S.; Gu, Y.; Kar, T. Evaluation of the H-bonding properties of CH···O interactions based upon NMR spectra. *J. Mol. Struct. (Theochem)* **2000,** *500*, 441-452.
99. Isaev, A. N. C-H···O, OH···C, and C-H···C interactions in complexes of carbocations and carboanions. *Russ. J. Inorg. Chem.* **2013,** *58*, 817-823.

FIGURE CAPTIONS

Fig 1. Optimized geometries (MP2/aug-cc-pVDZ) of a) $S(Me)_2$, b) $S(Me)_3^+$, c) $N(Me)_3$, and d) $N(Me)_4^+$ complexes with NMA as H bond acceptor. Blue numbers represent counterpoise-corrected binding energies in kcal/mol. Distances in Å and angles in degrees.

Fig 2. Binding energies plotted against Onsager function (F_o) for $S(Me)_2$, $S(Me)_3^+$, $N(Me)_3$ and $N(Me)_4^+$ complexes with NMA as proton acceptor, as MP2/aug-cc-pVDZ level. Yellow and blue colors indicate S and N donors, respectively, solid curves for cationic and dotted for neutral complexes. Red line represents neutral water dimer.

Fig 3. Optimized geometries (M06-2X/6-31+G**) for S^+ and N^+ complexes with elongated alkyl groups; NMA as proton acceptor. Blue numbers indicate counterpoise-corrected binding energies in kcal/mol. Distances in Å and angles in degrees.

Fig 4. Variation of binding energy with increase in alkyl chain length of R_3S^+ (yellow) and R_4N^+ (blue) complexes with NMA. Solid lines represent trifurcated CH···O H bonding with one CH of each of three terminal CH_3 groups; dotted lines indicate O interacting with the three CH_2 groups closest to central S or N atom.

Fig 5. Electrostatic potential maps for alkyl-substituted S^+ and N^+ monomers. Contours range from 0.20 - 0.25 au. Blue and red colors indicate most and least positive regions, respectively, on the van der Waals atomic surface.

Fig 6. Electron density shifts arising from formation of each complex: proton donor is listed, and NMA is proton acceptor in all cases. Blue regions indicate density increase, and red a density loss. Contours are shown at the 0.0005 au level.

Fig 7. Variation of binding energy for cationic complexes with increase in alkyl chain length. Broken curves were generated when all three CH donors arise from the same terminal methyl group; a single CH··O H-bond is characterized by solid curves. N donors are indicated by blue, and S by yellow.

Table 1. Binding energies (kcal/mol) of complexes with NMA computed at two levels of theory

proton donor	MP2/aug-cc-pVDZ	M06-2X/6-311+G**
$S(Me)_2$	4.88	6.26
$S(Me)_3^+$	20.55	22.17
$N(Me)_3$	2.05	2.83
$N(Me)_4^+$	18.79	20.29

Table 2. R(H··O) distances (Å) in complexes of NMA with terminal methyl groups, at M06-2X/6-31+G** level.

proton donor	binding E, kcal/mol	R(H···O), Å		
		Me-1	Me-2	Me-3
$S(Me)_2$	6.26	2.385	2.457	
$S(Me)_3^+$	22.17	2.162	2.188	2.192
$S(Et)_3^+$	15.00	2.254	2.258	2.279
$S(Pr)_3^+$	10.71	2.420	2.442	2.473
$N(Me)_3$	2.83	2.605	2.633	2.941
$N(Me)_4^+$	20.29	2.205	2.214	2.23
$N(Et)_4^+$	14.10	2.265	2.268	2.273
$N(Pr)_4^+$	10.47	2.385	2.385	2.402

Table 3: NBO values of E(2) (kcal/mol) for complexes involving terminal methyl groups, at M06-2X/6-31+G** level.

proton donor	$O_{lp}\rightarrow \sigma^*$(C-H) ($\pi CO\rightarrow \sigma^*$(C-H))			Total
	Me-1	Me-2	Me-3	
$S(Me)_2$	1.29(0.59)	1.72(0.84)		4.44
$S(Me)_3^+$	4.82(1.03)	3.72(1.81)	6.65(0.18)	18.21
$S(Et)_3^+$	3.25(1.00)	3.59(0.52)	4.54(0.06)	12.96
$S(Pr)_3^+$	1.51	1.20(0.26)	1.09(0.10)	4.16
$N(Me)_3$	0.54(0.56)	0.86(0.41)		2.50
$N(Me)_4^+$	3.81(0.92)	3.11(1.18)	5.27(0.06)	14.35
$N(Et)_4^+$	4.30(0.06)	3.00(1.04)	3.75(0.39)	12.54
$N(Pr)_4^+$	2.21	1.60(0.34)	1.77(0.20)	6.12

Table 4: SAPT decomposition of total binding energies (kcal/mol) of S and N complexes with NMA as H-bond acceptor.

	$S(Me)_2$	$N(Me)_3$	$S(Me)_3^+$	$N(Me)_4^+$
ES	-7.39	-3.32	-25.23	-22.60
EX	10.47	7.25	14.50	12.44
IND	-4.57	-3.26	-8.38	-7.01
IND+EXIND	-1.26	-0.66	-5.50	-4.73
DISP	-8.56	-6.53	-7.29	-6.48
DISP+EXDISP	-7.31	-5.60	-6.20	-5.55

Table 5: Changes in NMR chemical shielding (σ, ppm) of protons caused by complexation with NMA at M06-2X/6-31+G** level.

	terminal CH_3[a]	CH adjacent to S/N[b]	average of all H[c]	single $CH_3\cdot\cdot O$[d]	single $CH\cdot\cdot O$[e]
$S(Me)_2$	-0.74	-0.74	-0.09	-0.46	-1.91
$S(Me)_3^+$	-2.23	-2.23	-0.44	-0.79	-3.50
$S(Et)_3^+$	-1.73	-2.12	-0.41	-0.52	-2.98
$S(Pr)_3^+$	-1.15	-2.11	-0.33	-0.51	-2.49
$N(Me)_3$	-0.82	-0.82	-0.07	-0.46	-1.36
$N(Me)_4^+$	-2.01	-2.01	-0.45	-0.70	-3.22
$N(Et)_4^+$	-1.76	-1.78	-0.46	-0.52	-2.99
$N(Pr)_4^+$	-1.46	-1.92	-0.44	-0.56	-2.50

[a]average of only bridging H atoms, with NMA H-bonded to multiple terminal methyl groups
[b]average of only bridging H atoms, with NMA H-bonded to methylene groups adjacent to central atom
[c]average change of *all* H atoms, bridging and non-bridging, of terminal methyl groups H-bonded to NMA
[d]average of bridging H atoms, with NMA H-bonded to 3 H atoms of a single methyl group
[e]NMA H-bonded to a single H atom in a linear CH··O arrangement

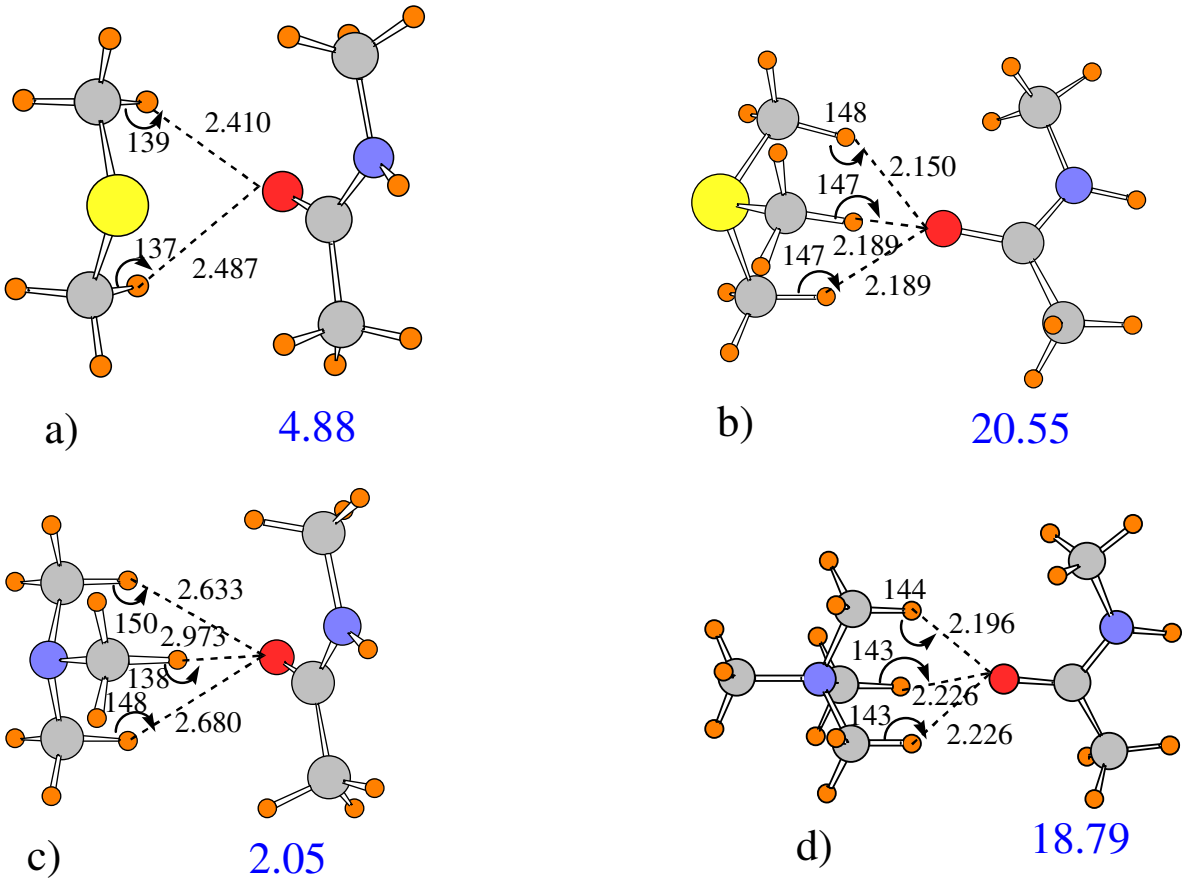

Fig 1. Optimized geometries (MP2/aug-cc-pVDZ) of a) $S(Me)_2$, b) $S(Me)_3^+$, c) $N(Me)_3$, and d) $N(Me)_4^+$ complexes with NMA as H bond acceptor. Blue numbers represent counterpoise-corrected binding energies in kcal/mol. Distances in Å and angles in degrees.

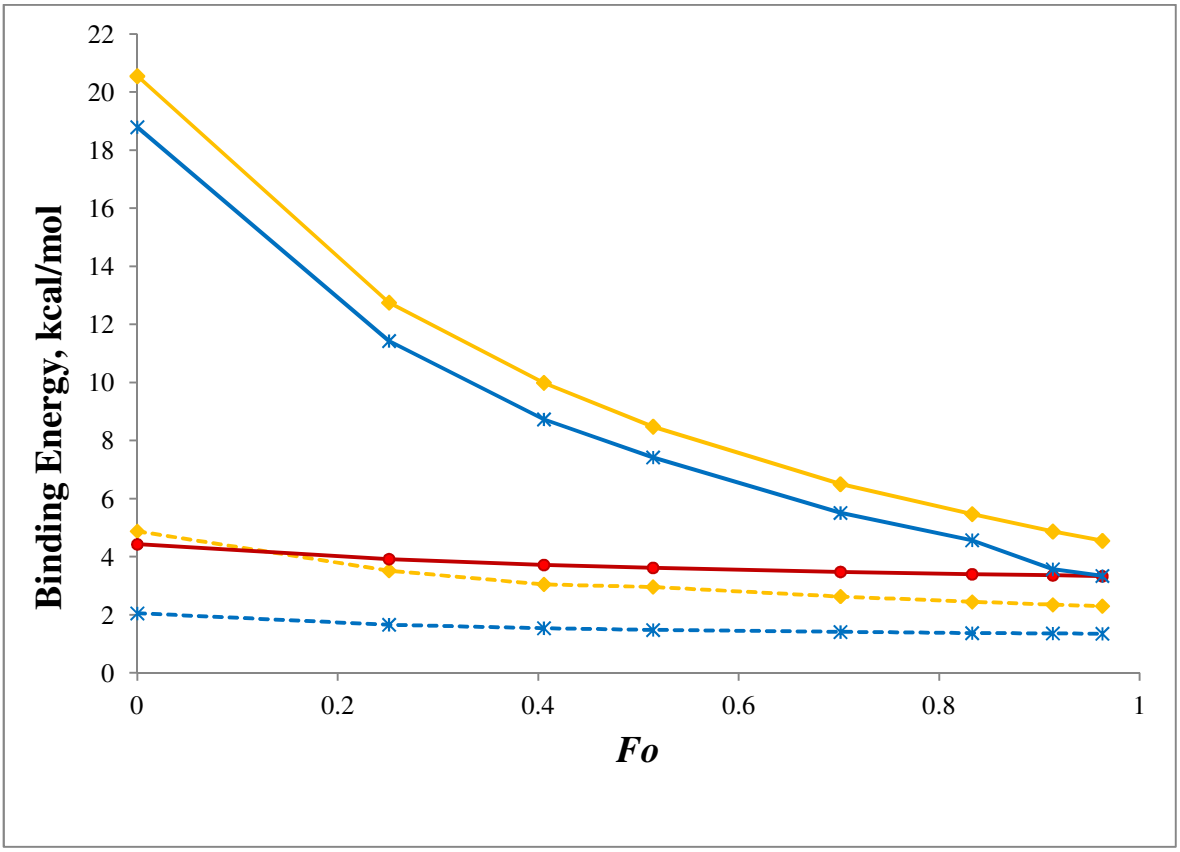

Fig 2. Binding energies plotted against Onsager function (F_o) for $S(Me)_2$, $S(Me)_3^+$, $N(Me)_3$ and $N(Me)_4^+$ complexes with NMA as proton acceptor, as MP2/aug-cc-pVDZ level. Yellow and blue colors indicate S and N donors, respectively, solid curves for cationic and dotted for neutral complexes. Red line represents neutral water dimer.

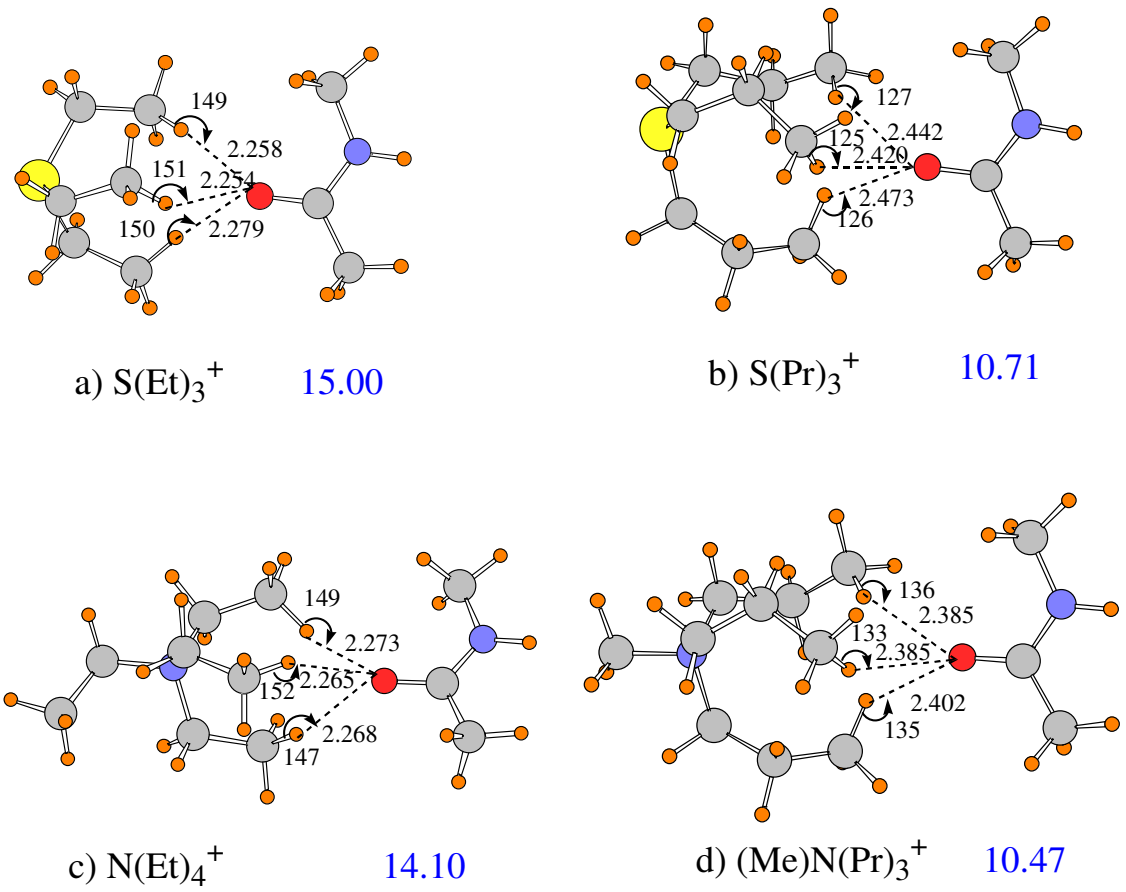

Fig 3. Optimized geometries (M06-2X/6-31+G**) for S^+ and N^+ complexes with elongated alkyl groups; NMA as proton acceptor. Blue numbers indicate counterpoise-corrected binding energies in kcal/mol. Distances in Å and angles in degrees.

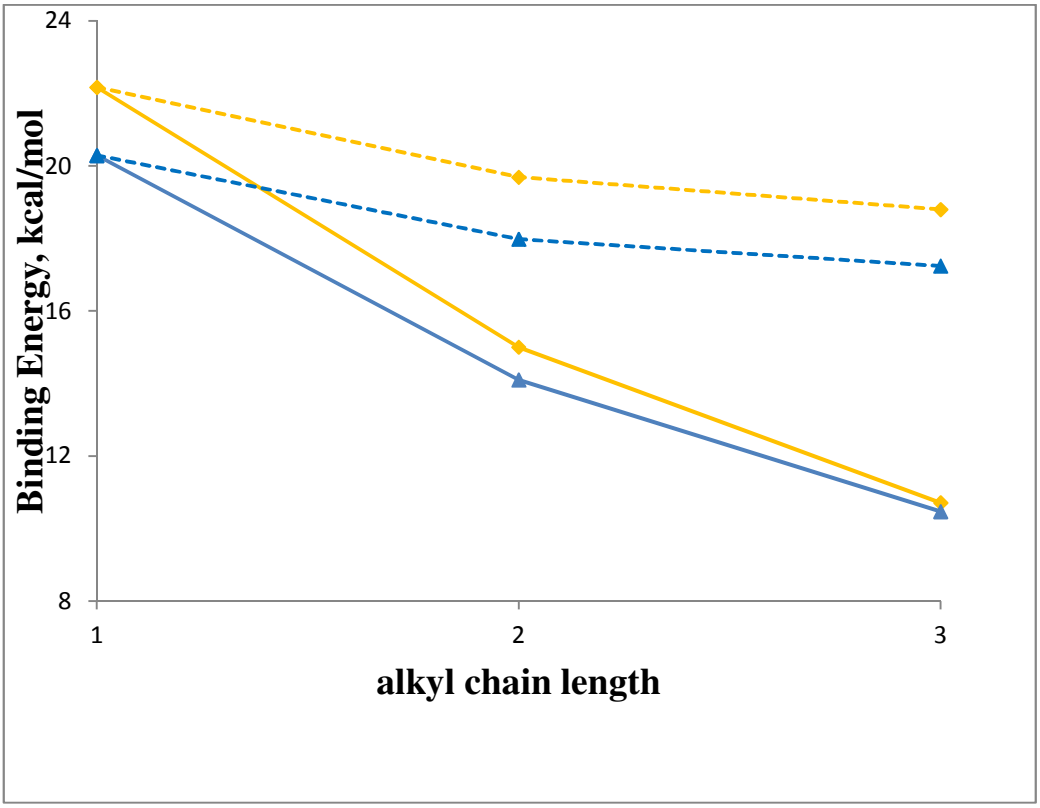

Fig 4. Variation of binding energy with increase in alkyl chain length of R_3S^+ (yellow) and R_4N^+ (blue) complexes with NMA. Solid lines represent trifurcated CH···O H bonding with one CH of each of three terminal CH_3 groups; dotted lines indicate O interacting with the three CH_2 groups closest to central S or N atom.

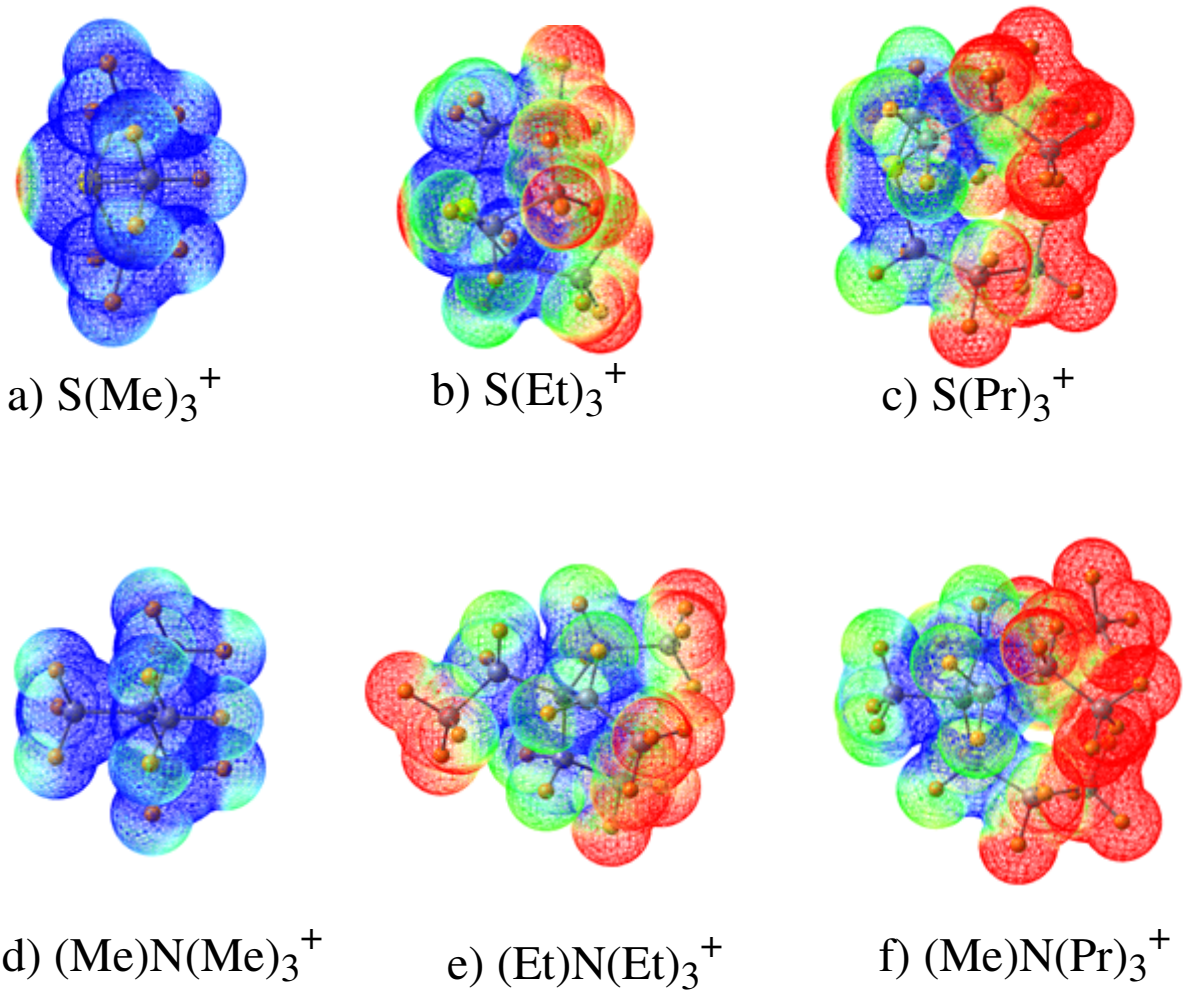

Fig 5. Electrostatic potential maps for alkyl-substituted S^+ and N^+ monomers. Contours range from 0.20 - 0.25 au. Blue and red colors indicate most and least positive regions, respectively, on the van der Waals atomic surface.

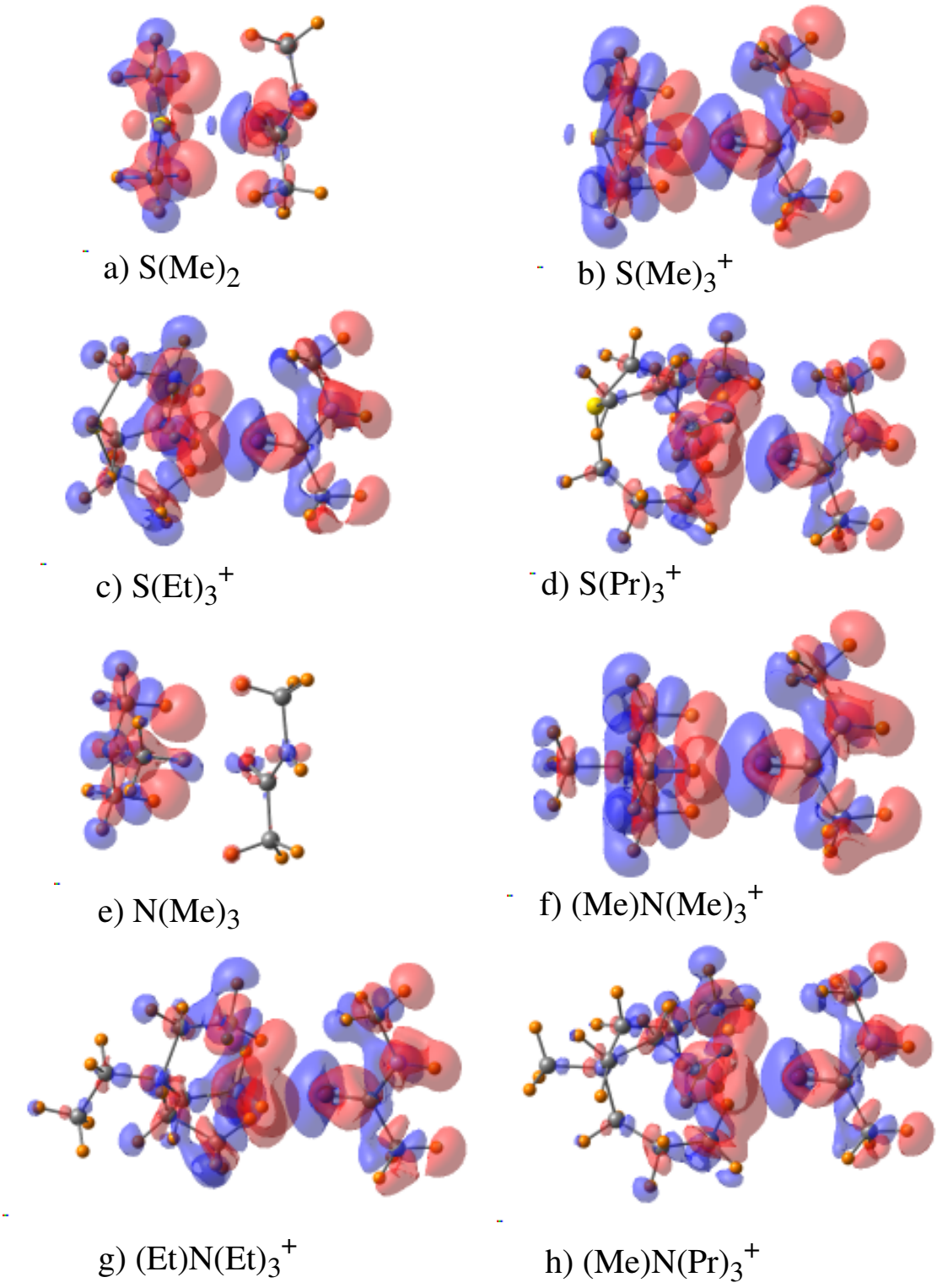

Fig 6. Electron density shifts arising from formation of each complex: proton donor is listed, and NMA is proton acceptor in all cases. Blue regions indicate density increase, and red a density loss. Contours are shown at the 0.0005 au level.

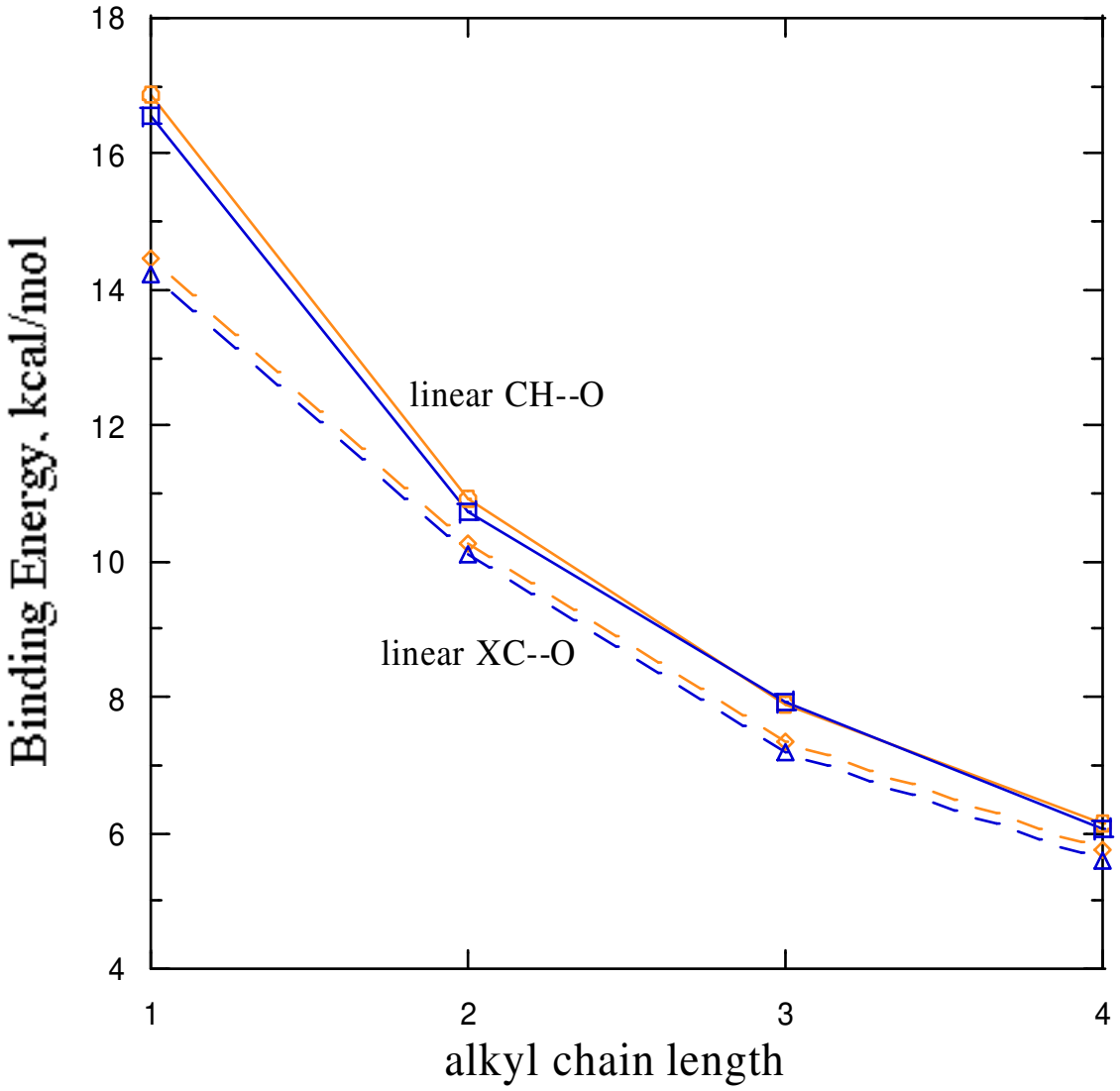

Fig 7. Variation of binding energy for cationic complexes with increase in alkyl chain length. Broken curves were generated when all three CH donors arise from the same terminal methyl group; a single CH··O H-bond is characterized by solid curves. N donors are indicated by blue, and S by yellow.

TOC Graphic: